RSC Advances

PAPER

View Article Online
View Journal | View Issue

Cite this: *RSC Adv.*, 2022, **12**, 32338

Examining computationally the structural, elastic, optical, and electronic properties of $CaQCl_3$ (Q = Li and K) chloroperovskites using DFT framework

Mudasser Husain,[a] Nasir Rahman,[*a] Hind Albalawi,[b] Safa Ezzine,[cj] Mongi Amami,[c] Tahir Zaman,[d] Altaf Ur Rehman,[e] Mohammad Sohail,[a] Rajwali Khan,[a] Abid Ali Khan,[f] Tahir[g] and Aurangzeb Khan[hi]

This study presents the investigations of structural, elastic, optical, and electronic properties of $CaQCl_3$ (Q = Li and K) chloroperovskites for the first time using the DFT framework. The WIEN2K and IRelast packages are used in which the exchange–correlation potential of the modified Becke–Johnson potential (TB-mBJ) is used for obtaining better results. The optimized crystal structural parameters comprising the lattice constant, optimum volume, ground state energy, bulk modulus, and the pressure derivative of bulk modulus are computed by fitting the primitive unit cell energy *versus* primitive unit cell volume using the Birch–Murnaghan equation of state. The elastic properties which consist of cubic elastic constants, Poisson's ratio, elastic moduli, anisotropy factor, and the Pugh ratio are computed using the very precise IRelast package incorporated inside WIEN2K. The electronic properties are analyzed from the computation of electronic bands structure and density of states (DOS), and it is concluded that an indirect band gap of 4.6 eV exists for $CaLiCl_3$ and a direct band gap of 3.3 eV for $CaKCl_3$ which confirms that $CaLiCl_3$ is an insulator while $CaKCl_3$ is a wide band gap semiconductor. The analysis of DOS shows that the greater contribution to the conduction band (CB) occurs because of the "Ca" element whereas in the valence band the major contribution is from the "Cl" element. The spectral curves of various parameters of optical properties from 0 eV up to 42 eV incident photon energies are observed and it is found that the $CaQCl_3$ (Q = Li and K) chloroperovskites are optically active having a high absorption coefficient, optical conductivity, optical reflectivity, and energy loss function from 25 eV to 35 eV incident photon energies. The applications of these materials can be deemed to alter or control electromagnetic radiation in the ultraviolet (UV) spectral regions. In summary, the results for selected $CaQCl_3$ (Q = Li and K) chloroperovskites depict that these are important compounds and can be used as scintillators, and energy storage devices, and in many modern electronic gadgets.

Received 7th September 2022
Accepted 3rd November 2022

DOI: 10.1039/d2ra05602j

rsc.li/rsc-advances

1. Introduction

Discovering the physical properties of materials for practical use has consistently remained a major area of research. Even in a scientifically equipped society, materials scientists are always searching for the best and most effective materials. Perovskites have drawn a lot of interest because of their important applications in optical devices,[1–3] energy storage,[4] and semiconducting industries.[5–9] Researchers in materials science have studied the perovskite materials using DFT[10–13] and a wide variety of substances are found in the perovskites family, ranging from insulators to superconductors and from diamagnetic to colossal magnetoresistive (CMR) substances. Perovskite materials are also preferred as lens materials since they do not exhibit the birefringence that makes lens design challenging.[14] The common chloroperovskite structure is $ABCl_3$, where "A" and "B" represents alkali metals and alkaline earth metals respectively, whereas "Cl"

[a]*Department of Physics, University of Lakki Marwat, 28420, Lakki Marwat, KPK, Pakistan. E-mail: nasir@ulm.edu.pk*

[b]*Department of Physics, College of Sciences, Princess Nourah bint Abdulrahman University (PNU), P.O. Box 84428, Riyadh 11671, Saudi Arabia*

[c]*Department of Chemistry, College of Sciences, King Khalid University, Abha, Saudi Arabia*

[d]*Department of Mathematics, Government Post Graduate College, Karak, KPK, Pakistan*

[e]*Department of Physics, Riphah International University, Lahore 54000, Pakistan*

[f]*Department of Chemical Sciences, University of Lakki Marwat, 28420, Lakki Marwat, KPK, Pakistan*

[g]*Department of Physics, Pontificia Universidade Católica do Rio de Janeiro, Rua Marques de São Vicente, 22451-900 Rio de Janeiro, Brazil*

[h]*Department of Physics, Abdul Wali Khan University, Mardan, 23200, KPK, Pakistan*

[i]*University of Lakki Marwat, 28420, Lakki Marwat, KPK, Pakistan*

[j]*Laboratoire des Matériaux et de L'Environnement Pour le Développement Durable LR18ES10, 9 Avenue Dr. Zoheir Sai, Tunis 1006, Tunisia*

is the chlorine element. Chloroperovskites possess striking properties, specifically lead-containing chloroperovskites, and have possible use in the optical and electronic industries. The chloroperovskites usually hold a very large band gap due to which its applications can be deemed in many modern energy storage devices. The nature of wide-band-gap energy is suitable for it to absorb or emit ultraviolet (UV) light in applications of optoelectronic devices. Energy storage is a crucial component of a large number and variety of electronic devices, particularly for mobile devices and electric or hybrid vehicles. According to the literature, chloroperovskites are more stable than other halides perovskites.[15–17] Due to their special characteristics of tunable laser,[18] electron–phonon interactions,[19,20] crystal fields,[21] ferroelectricity,[22] phase transition behaviors,[23] antiferromagnetism,[24] semiconductivity,[25] and as a scintillating material,[26] the perovskite compounds have a comprehensive range of applications. The high intensity, high directivity, and high energy[27] scintillating materials and scintillators are widely employed in a variety of applications,[28,29] including healthcare (medical imaging),[30] calorimetry in high energy physics, territorial security,[31] industrial screening,[32] and astronomy.[33] Scintillators are substances that may convert ionizing "X" or photons into light that is visible or almost visible (near ultraviolet). The light emitted will be transformed into an electrical signal that can then be examined depending on the applications.[34,35] As a result of high band gaps, high absorption coefficients, and economical manufacturing, chloroperovskite has recently been regarded as a scintillating material.[36–38] After extensive research on chloroperovskites, we conclude that the existence of the "Ca" element in the ternary $CaQCl_3$ (Q = Li and K) choloroperovskites shows a significant role in structural, elastic, and optoelectronic properties. Nowadays the DFT is proven to be the most precise and accurate tool for the computation of different various physical properties of a material.[39–41] This research intends to provide the first insight into some of the fundamental physical properties of ternary $CaQCl_3$ (Q = Li and K) chloroperovskites for the first time using the DFT framework for the possible applications in energy-storing devices, scintillating materials, and many modern technological devices.

2. Computational methodology

The presented research is done using the WIEN2K[42] simulation code to carry out the plane-wave and self-consistent (PWSCF) approach, which is based on DFT (density functional theory).[43] For the crystal structural optimization, the generalized gradient approximation of Perdew–Burke–Ernzerhof (GGA-PBE)[44] is employed to compute the fundamental structural properties and elastic properties. The IRelast package[45] is used for the computations of different parameters of elastic properties. The exchange–correlation potential of the modified Becke–Johnson potential (TB-mBJ)[46] is used for obtaining better results for electronic properties (*i.e.* band gap and DOS) and optical properties. The number of 2000 *K*-points is used to sample the first Brillouin zone in reciprocal space. To attain a reasonable degree of convergence, this study takes into account some FP-LAPW basis functions up to RMT × K_{max} (where RMT is the minimum radius of the muffin-tin spheres equal to 8 and K_{max} specifies the magnitude of the biggest *k*-vector in the plane wave expansions). The RMT values are chosen for each atom in such a way that there is no overlap and the muffin-tin radii "RMT" for constituent atomic spheres are 2.5, 1.78, and 1.92 atomic units (a. u.) for "Ca", "Q" where (Q = Li and K), and "Cl", respectively. The self-consistent field (SCF) computations are observed to have met at 0.001 mRy total energy. The optical properties are computed from the basic complex dielectric function of the form $\varepsilon(w) = \varepsilon_1(w) + i\varepsilon_2(w)$.[47] The xcrysden,[48] Gnuplot,[49] origin[50] and xmgrace[51] are mainly used in research for graphing purpose. The aforementioned computational is employed for the first insight into some of the physical properties including structural, elastic, optical, and electronic properties of ternary $CaQCl_3$ (Q = Li and K) choloroperovskites.

3. Results and discussion

This portion describes and presents in detail the results obtained for ternary $CaQCl_3$ (Q = Li and K) choloroperovskites using the research methodology presented above. Each physical property is discussed here one by one.

3.1 The structural properties

To access other physical properties (such as electrical, optical, and elastic), the investigation of structural properties for these materials is a crucial stage in the *ab initio* simulation analysis. In this section, we used the GGA-PBE approximation to examine the structural characteristics of $CaQCl_3$ (Q = Li and K) chloroperovskites belonging to the space group-221 ($Pm\bar{3}m$). The primitive crystalline unit cell of both the $CaQCl_3$ (Q = Li and K) chloroperovskites are depicted in Fig. 1. Both the crystalline unit cell has five (5) atoms, where Ca at Wyckoff positions of (0, 0, 0), Q = Li and K lies at (0.5 0.5 0.5), and Cl positioned at (0, 0.5 0.5). The tolerance factor "τ" is computed for the selected chloroperovskites and found to be 0.94 for $CaKCl_3$ and 0.98 for $CaLiCl_3$, which confirms the cubic structure of the compounds. The fundamental structural parameters including the unit cell optimum volume, unit cell optimum energy, optimized lattice constant, pressure derivative of bulk modulus, and bulk modulus, are determined by fitting the primitive unit cell energy as a function of primitive unit cell volume using the Birch–Murnaghan equation of state,[52] as described as:

$$E\ (\mathrm{V}) = E_0 + \frac{B}{B'(B'-1)}\left[V\left(\frac{V_0}{V}\right)^{B'} - V_0\right] + \frac{B}{B'}(V - V_0) \quad (1)$$

where in the equation above E_0, B, B', V, and V_0 are respectively, the optimum value of total energy, the bulk modulus, the pressure derivative of bulk modulus, the total unit cell volume, and the optimized unit cell volume.

The structural optimization curves computed using the GGA approximation are depicted in Fig. 2, and the optimized values that are obtained from the Birch–Murnaghan fit curves are provided in Table 1.

The formation energies in the cubic phase of the ternary $CaQCl_3$ (Q = Li and K) chloroperovskites are calculated using

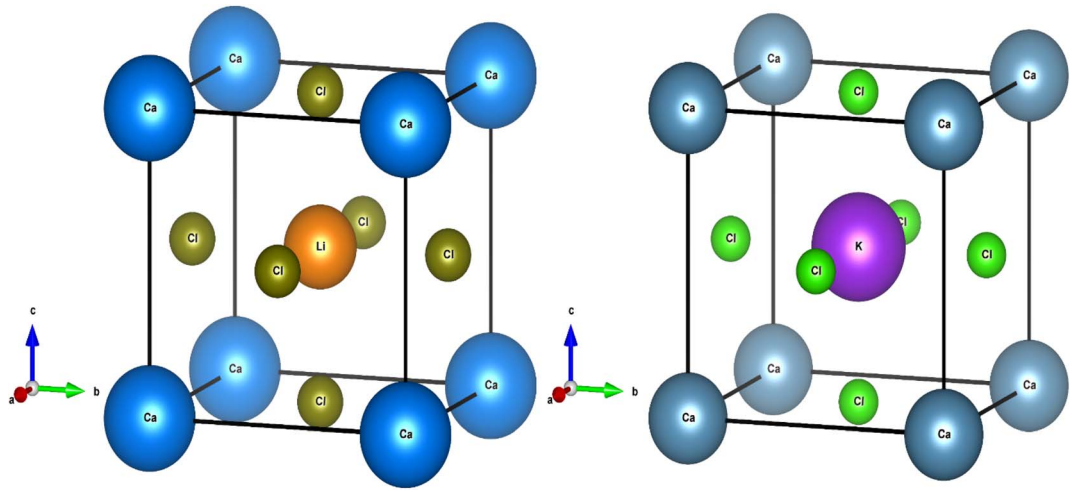

Fig. 1 The investigated crystal structures of $CaQCl_3$ (Q = Li and K) chloroperovskites.

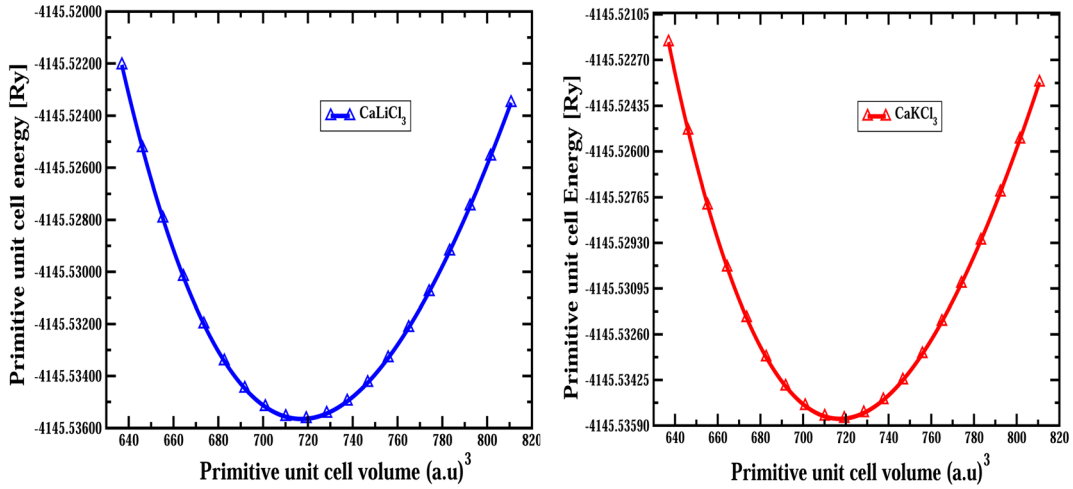

Fig. 2 The computed optimization of primitive unit cell volume *versus* primitive unit cell energy for $CaQCl_3$ (Q = Li and K) chloroperovskites in the cubic phase.

the expression below, which proved the chemical stability of the complex compounds.

$$\Delta H_f = E_{total}(CaQCl_3) - E_{Ca} - E_Q - 3E_{Cl} \quad (2)$$

where in the above eqn (2), ΔH_f is the formation energy, E_{total}($CaQCl_3$) is the total optimum energy of $CaQCl_3$ (Q = Li and K), E_{Ca} is the ground state energy of the "Ca" atom, E_Q shows the ground energy of Q = Li and K atoms and E_{Cl} shows the ground energy of chlorine atom. The values of the formation energies that are computed are listed in Table 1, and it is revealed that all the results are negative, indicating that ternary $CaQCl_3$ (Q = Li and K) chloroperovskites compounds may be synthesized experimentally.

3.1.1 Phonon dispersion curves. The phonon dispersion curves along the high symmetries points are computed for $CaQCl_3$ (Q = Li and K) chloroperovskites compounds for the sake of stability purposes. It is seen from the dispersion curves of the Fig. 3 that there exist negative peak dispersion curves below zero frequency limit, indicating that both the materials are unstable.

3.2 The electronic properties

A first-class study of the electronic band structure and DOS is interested in the electronic properties of a solid to ascertain the nature of chloroperovskite materials, including whether they are metals, semiconductors, or insulators, as well as the kinds of bonds that are formed between the various elements of these materials and their gap energies. After optimizing a material's structure utilizing a 2000 number of *k*-points in the first Brillouin zone, the band structure of the material can be ascertained using DFT calculations. According to the locations of high symmetry points that is "*M*–*Γ*" and "*Γ*–*Γ*" shown in Fig. 4, the band structures of both the examined ternary $CaQCl_3$ (Q = Li and K) chloroperovskites compounds are predicted through the TB-mBJ approximation in the Brillouin zone between −6 eV and +6 eV. The band structure for $CaLiCl_3$ shows that the

Table 1 The predicted optimized structural parameters include the lattice constant a_0 (Å), bulk modulus B (GPa), pressure derivative of bulk modulus B', optimum volume V_0 (a.u)^3, ground state energy E_0 (Ry), the formation energies ΔH_f (eV) and the tolerance factor "τ" for ternary $CaQCl_3$ (Q = Li and K) chloroperovskites

Optimized structural parameters	$CaKCl_3$	$CaLiCl_3$
a_0 (lattice constant) in Å	5.3795	4.6380
B (bulk modulus) in GPa	79.43	72.66
Pressure derivative of bulk modulus B' (GPa)	5.76	7.21
Optimum volume V_0 (a.u)^3	720.76	719.32
Ground state energy E_0 (Ry)	−4145.53	−4145.49
ΔH_f (eV)	−8.46	−7.93
τ	0.94	0.98

valence band's maximum (VBM) lies at "M" symmetry points, whereas the conduction band's minimal (CBM) is situated at the "Γ" symmetry points. We can infer from this analysis that the band structure has an indirect nature from "M–Γ" with a band gap "E_g" of 4.6 eV for $CaLiCl_3$ and thus act as an insulator. The band structure analysis for $CaKCl_3$ depicts a direct nature from "M–M" with a band gap "E_g" of 3.3 eV and displays the nature of a wide band gap semiconductor. Based on the predicted electronic band gap the application for these materials can be deemed in many energy storage devices and semiconducting industries.

The deep insight into the electronic properties of materials requires the analysis of DOS which includes TDOS and PDOS (total density of states and partial density of states) as displayed in the Fig. 3 within the energy range of −6 eV to 6 eV for $CaQCl_3$ (Q = Li and K) chloroperovskites. The horizontal red dotted line in both graphs at 0 eV shows the Fermi energy level (E_F). The portion of the graph that lies above the Fermi level is known as the conduction band (CB) whereas the portion below depicts the valence band (VB). The DOS describes deeply the contributions of different elemental electronic states to the "VB" and "CB". The dominant participation in the states of "VB" adjacent to the Fermi level is due to the "Li" elemental part, as shown by the magenta and by Li-p state for $CaLiCl_3$ and "K" and K-p state for $CaKCl_3$ in Fig. 4. The greater contribution in the states of the "CB" occurs from the "Ca" and Ca-d state elements for both the $CaQCl_3$ (Q = Li and K) chloroperovskites compounds. The larger band gap that exists in $CaLiCl_3$ material is because of the Ca-d and Li-p states and in $CaKCl_3$ is due to the Ca-d and K-p states. The electronic band gap depicted in DOS is fully consistent with the gap in the band structures for $CaQCl_3$ (Q = Li and K) chloroperovskites.

3.3 The optical properties

This section of results and discussion describe in very detail the different parameters associated with the optical properties of $CaQCl_3$ (Q = Li and K) chloroperovskites. As it is determined that the compounds $CaLiCl_3$ possess an insulating nature with an indirect band gap and $CaKCl_3$ with a direct wide band gap based on the electronic properties and using the band structure; as a result, these compounds are very suitable for optical applications. The following formulas are used to compute the reflectivity, refractive index, extinction coefficient, and absorption coefficient for several optical properties.[53]

$$\varepsilon(w) = \varepsilon_1(w) + i\varepsilon_2(w) \tag{3}$$

$$n(\omega) = \left[\frac{\varepsilon_1(w)}{2} + \frac{\sqrt{\varepsilon_1^2(\omega) + \varepsilon_2^2(\omega)}}{2}\right]^{\frac{1}{2}} \tag{4}$$

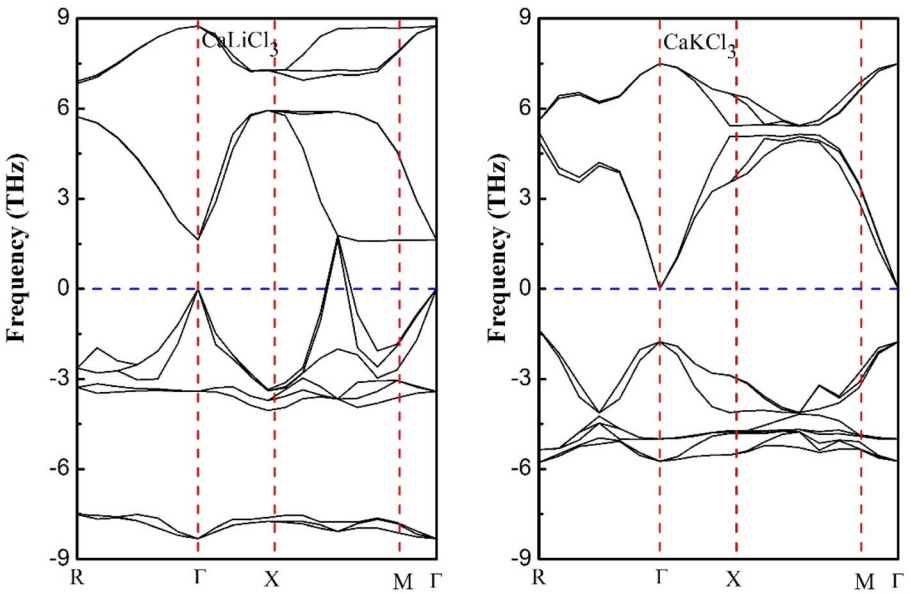

Fig. 3 Phonon dispersion curves at high symmetries points for ternary $CaQCl_3$ (Q = Li and K) chloroperovskites compounds.

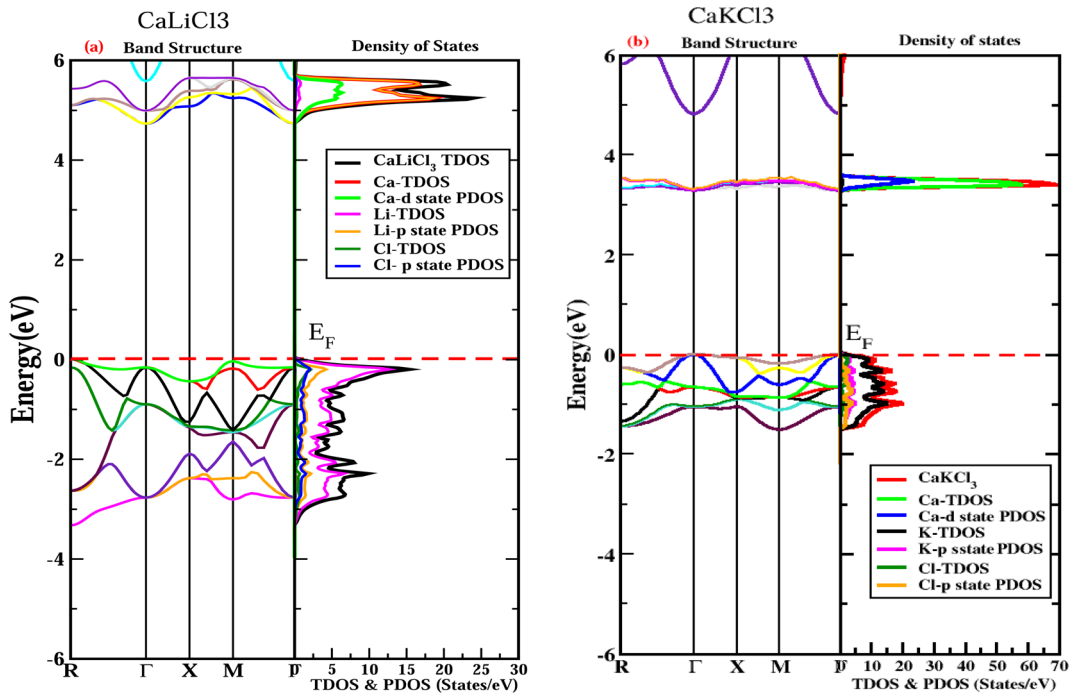

Fig. 4 The examined fitted electronic band structures and DOS for $CaQCl_3$ (Q = Li and K) chloroperovskites at high symmetries points in the first Brillion zone using TB-mBJ approximation.

$$k(\omega) = \left[\frac{-\varepsilon_1(w)}{2} + \frac{\sqrt{\varepsilon_1{}^2(\omega) + \varepsilon_2{}^2(\omega)}}{2}\right]^{\frac{1}{2}} \quad (5)$$

$$I(\omega) = \frac{2\omega}{c}k(\omega) \quad (6)$$

$$R(w) = \frac{(1-n)^2 + k^2}{(1+n)^2 + k^2} \quad (7)$$

$$\sigma(\omega) = \frac{2Wev\hbar(\omega)}{E_0} \quad (8)$$

All the fundamental optical properties are computed from the dielectric function in incident photon energies from 0 eV to 42 eV employing the TB-mBJ approach with an optimized lattice constant.

3.3.1 The dielectric function ($\varepsilon_1(w)$, $\varepsilon_2(w)$). The dielectric function is crucial for calculating optical properties since it defines the material's optical reaction at all photon energies. Optical dielectric constants are critical to modeling the

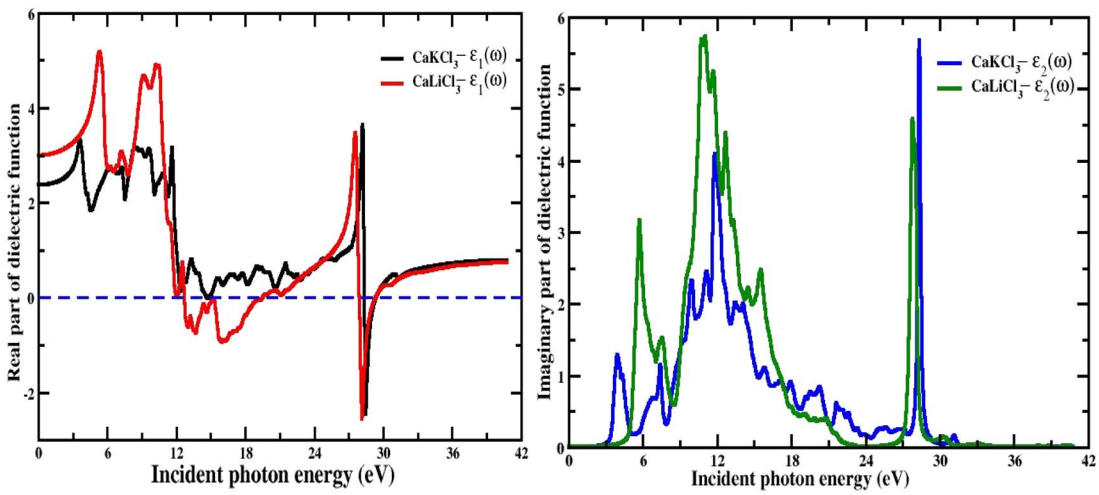

Fig. 5 The computed real and imaginary parts of dielectric function for $CaQCl_3$ (Q = Li and K) chloroperovskites.

electronic and optical properties of materials. The dielectric constant mainly improved the charge density of the materials. The real part represents the ability of the material to store the electric energy and is related to the polarization while the imaginary part is responsible for the damping of the wave and dissipation of energy. It is very clear in Fig. 5 of the real part of the dielectric function that the spectra for both materials are consistent with each other in terms of the pattern. The curves of "$\varepsilon_1(w)$" varies from 0 eV incident photon energy up to 42 eV, which shows that at the low range of photon energy the curve rises to a maximum positive peak of 5.3 for $CaLiCl_3$ and 3.7 for $CaKCl_3$. Both the $CaQCl_3$ (Q = Li and K) chloroperovskites achieve negative maximum values which shows polarization in these energy regions. The real static "$\varepsilon_1(0)$" dielectric function value for $CaLiCl_3$ is 3 and that for $CaKCl_3$ is 2.5. The analysis of the optical transition from the valence band to the conduction band requires the description and understanding of the imaginary part "$\varepsilon_2(w)$" of the dielectric function. The spectra of "$\varepsilon_2(w)$" for both the interesting materials are shown on the right side of Fig. 5. The maximum peaks that occur for both materials are 5.8 for $CaLiCl_3$ and 5.6 for $CaKCl_3$ in the photon energy range from 0 eV up to 42 eV. The maximum peaks of "$\varepsilon_2(w)$" spectra lie at a high energy photon range, which confirms that both ternary $CaQCl_3$ (Q = Li and K) chloroperovskites compounds possess a very good absorption of light in the ultraviolet range.

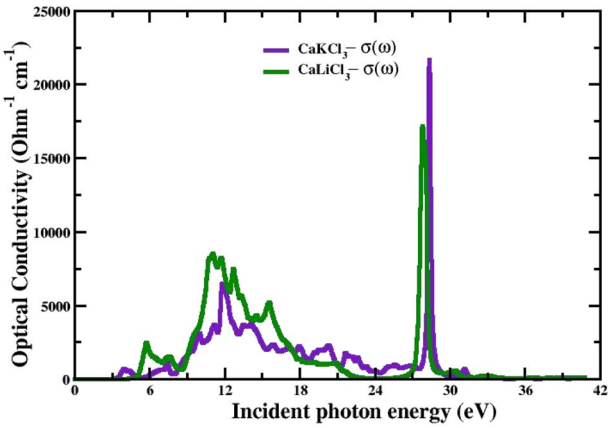

Fig. 6 The computed optical conductivity for $CaQCl_3$ (Q = Li and K) chloroperovskites.

3.3.2 The optical conductivity. The connection between the strength of the generated electric field's amplitude and the material's induced current density at a specified frequency is determined by the optical conductivity of a material. The computed optical conductivity spectral curves for both the ternary $CaQCl_3$ (Q = Li and K) chloroperovskites compounds are presented in the Fig. 6 within the incident photon energy ranges from 0 eV up to 42 eV. It is very clear in the Fig. 6 that the optical conductivity starts at the incident photon energy levels which is consistent with the electronic band gap energy. The maximum optical conductivity for $CaLiCl_3$ reaches 22 200 Ohm^{-1} cm^{-1} at 28 eV photon energy while that for $CaKCl_3$ is 17 250 Ohm^{-1} cm^{-1} at 26 eV incident photon energy. Both ternary $CaQCl_3$ (Q = Li and K) chloroperovskites compounds possess high optical conductivity at the high energy level, which gives a clue that these materials can be used in the ultraviolet range in optical devices.

3.3.3 The absorption Co-efficient. It is determined using eqn (6) and is identified as the amount of light intensity absorbed in a unit length of the material.[54] Fig. 7, which depicts the absorption coefficient spectrum generated from the TB-mBJ approximation, describes the behavior of the $I(w)$ (absorption

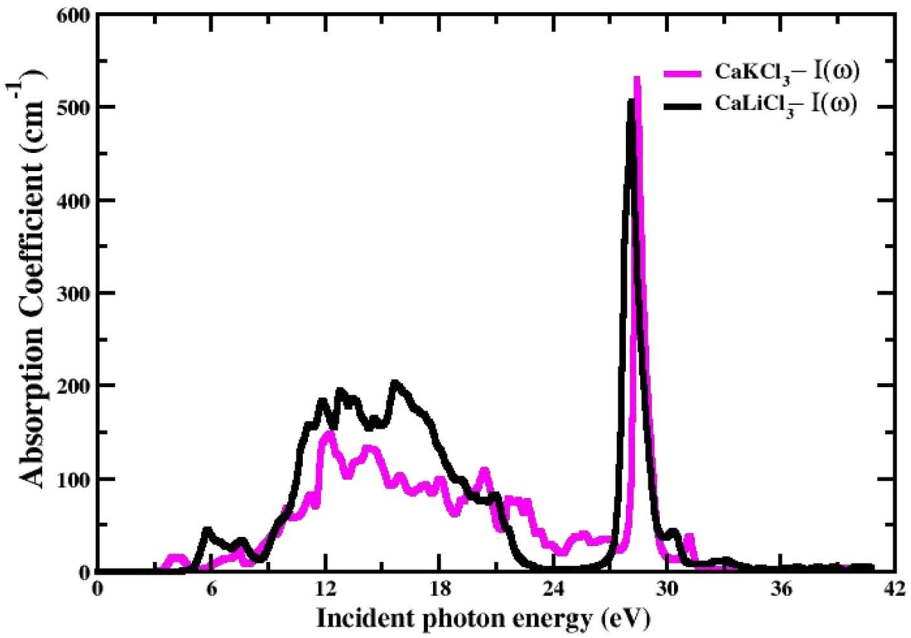

Fig. 7 The computed absorption coefficient for $CaQCl_3$ (Q = Li and K) chloroperovskites.

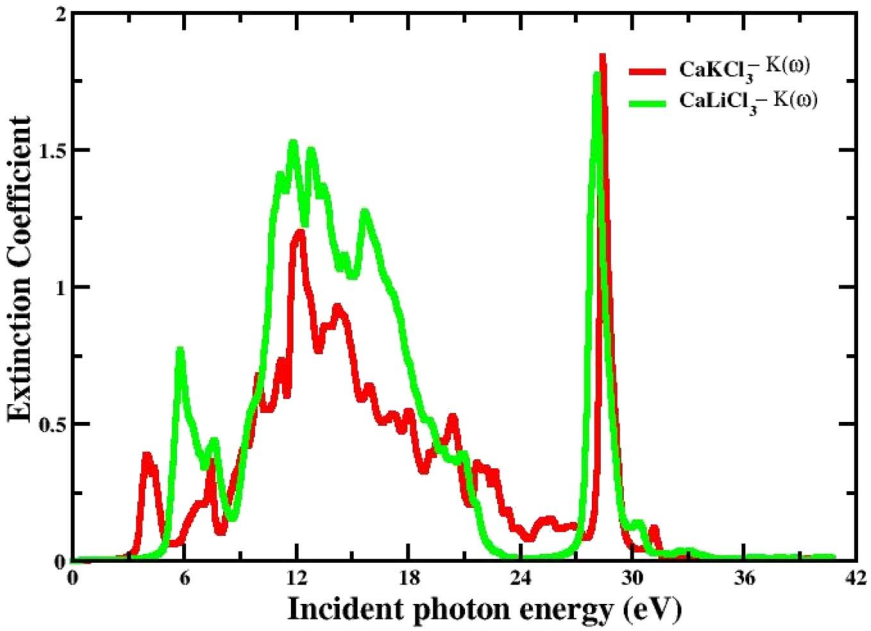

Fig. 8 The computed extinction co-efficient for $CaQCl_3$ (Q = Li and K) chloroperovskites.

coefficient) and how it behaves similarly to the dielectric constant $\varepsilon(w)$. We observe that there is no light absorption below the threshold energy, which is very expected given that below the bands, we are unable to induce electronic band transitions from the valence to the conduction band.[55] The critical values of $I(w)$ for both the $CaQCl_3$ (Q = Li and K) chloroperovskites are higher than the values of the band gap measured from the band structure. The maximum absorption peak that occurs is 527 cm^{-1} for $CaKCl_3$ and 521 cm^{-1} for $CaLiCl_3$ at incident photon energies of 28 eV and 26 eV respectively which are more useful at ultraviolet ranges.

3.3.4 The extinction co-efficient. The spectrum of extinction coefficient $K(\omega)$, investigated for the selected $CaQCl_3$ (Q = Li and K) chloroperovskites materials are presented in Fig. 8 within the incident photon energy from 0 eV up to 42 eV. The high values of $K(\omega)$ in the shorter wavelength range indicate that these films are opaque in this range since the extinction coefficient $K(\omega)$, is a measure of the amount of light lost owing to scattering and absorption per unit volume. The curve's oscillatory form results from an interference effect that manifests at longer wavelengths. It is very clear from Fig. 8 that both the materials are opaque in the lower range of incident photon energies and the interference effect is observed at the longer wavelengths regions.

3.3.5 The refractive index. The refractive index $n(\omega)$, which is determined by eqn (4) and is directly related to the real dielectric function, describes the speed of light propagation at the density of the material and is related directly to the real part of the dielectric function "$\varepsilon_1(w)$". Fig. 9 shows the computed curves of "$\varepsilon_1(w)$" in the incident photon energy of 0 eV to 42 eV for ternary $CaQCl_3$ (Q = Li and K) chloroperovskites. The static refractive index $n(0)$ for both compounds is 1.75 for $CaLiCl_3$ and 1.58 for $CaKCl_3$. As can be seen from the Fig. 9 that the refractive index goes on increasing and decreasing patterns while increasing the incident photon energy. The maximum peak of $n(\omega)$ occurs for $CaLiCl_3$ is 2.48 and that for $CaKCl_3$ is 2.25.

3.3.6 The optical reflectivity. The power reflected at a material's surface is defined as reflectivity. Fig. 10 shows the $R(w)$ given by eqn (7) and the obtained spectral curves of $R(w)$ for the $CaQCl_3$ (Q = Li and K) chloroperovskites. The static values of $R(0)$ for $CaQCl_3$ (Q = Li and K) are 0.05 for $CaKCl_3$ and 0.08 for $CaLiCl_3$ respectively. The optical reflectivity is very small in the photon energies ranging from 0 eV to 5 eV and further increasing the photon energy the $R(w)$ spectra increases for both the compounds reaches to maximum values of 0.74 for $CaLiCl_3$ and 0.63 for $CaKCl_3$ at the high photon ultraviolet energy ranges.

3.3.7 The energy loss function. The spectrum of energy loss function $L(w)$ that characterize inelastic scattering computed for the ternary $CaQCl_3$ (Q = Li and K) chloroperovskites materials from 0 eV to 42 eV incident photon energy is depicted in Fig. 11. The higher peaks at the high incident photon energy in the $L(w)$ spectra determine the Plasmon energy of these perovskite compounds. The energy loss function reveals the reaction of a solid to an external electromagnetic perturbation.

3.4 The elastic properties

Research on elastic characteristics is crucial as it provides evidence about the mechanical stability and type of bonding nature of solids materials. The elastic constants for a cubic crystal can be determined using the IRelast package[45] and are merely reduced to the three constants C_{11}, C_{12}, and C_{44}. These constants can be utilized to relate the mechanical reaction to the material's ductility or fragility during an elastic domain deformation. In this research, we used the GGA approach to examine the elastic constants for the ternary $CaQCl_3$ (Q = Li and

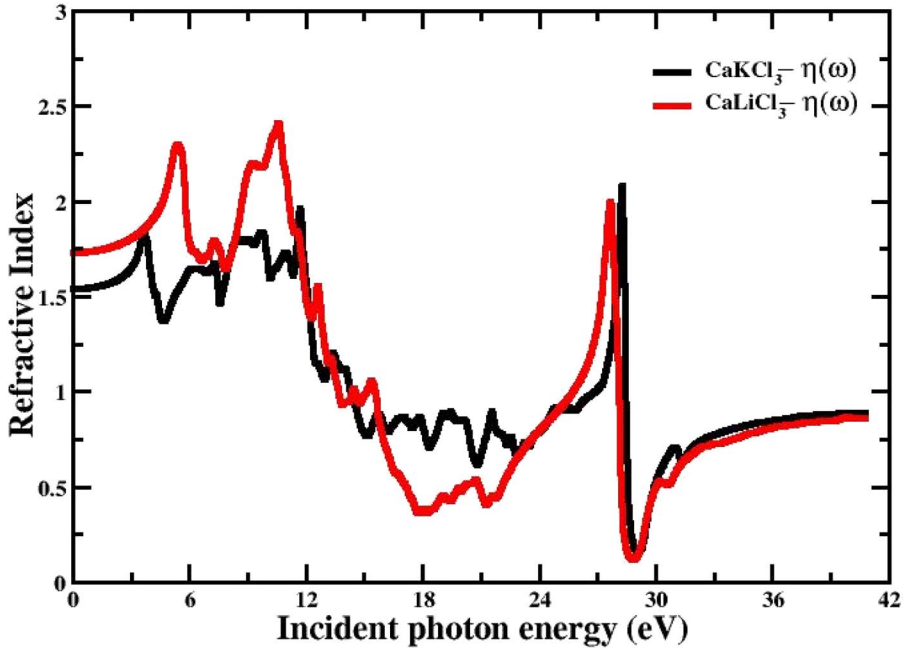

Fig. 9 The computed refractive index for $CaQCl_3$ (Q = Li and K) chloroperovskites.

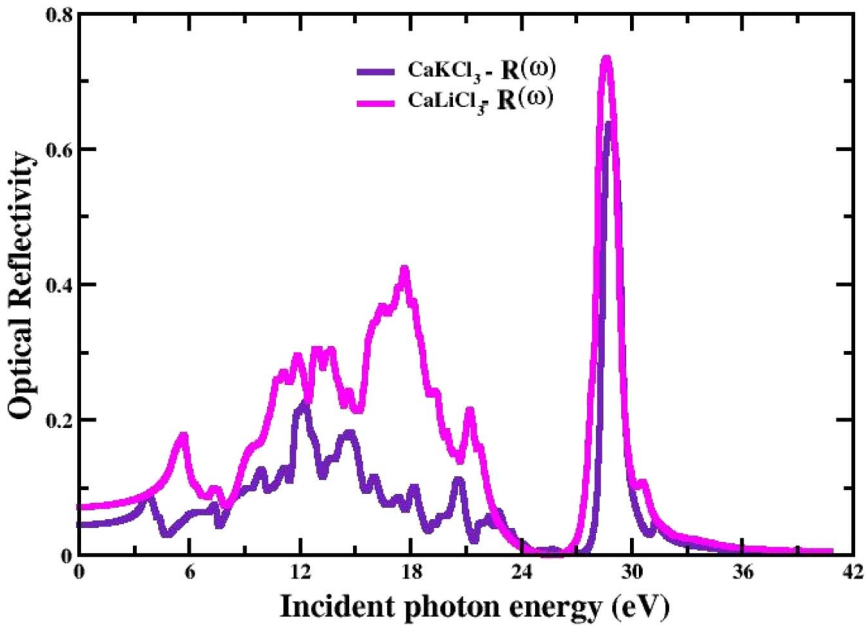

Fig. 10 The computed optical reflectivity for $CaQCl_3$ (Q = Li and K) chloroperovskites.

K) chloroperovskites compounds under typical conditions of the simple cubic structure. Using the IRelast package the investigated elastic constants, and other mechanical parameters are summarised in Table 2. The findings unmistakably demonstrate that both of the chloroperovskite materials under investigation exhibit higher compression resistance due to their substantial values of C_{11} (64.84 GPa) in comparison to C_{12} (45.76 GPa) and C_{44} (32.56 GPa) for $CaLiCl_3$ and for $CaKCl_3$ the values are C_{11} (87.74 GPa) compared to C_{12} (56.26 GPa) and C_{44} (38.86 GPa). The investigated elastic constants are positive and the Born–Huang mechanical stability criteria[56] $C_{11} > 0$, $C_{12} > 0$, $C_{44} > 0$, $C_{11} + 2C_{12} > 0$, $C_{11} - C_{12} > 0$, and $B > 0$ predict that both the selected compounds are stable mechanically. We determined two crucial parameters, such as the bulk modulus "B" and the shear modulus "G", to examine the behavior of a material that either is ductile/brittle. Both "B" and "G" in general are calculated using Voigt and Reuss's estimations.[57] The following formulas provide the compressibility modulus and shear

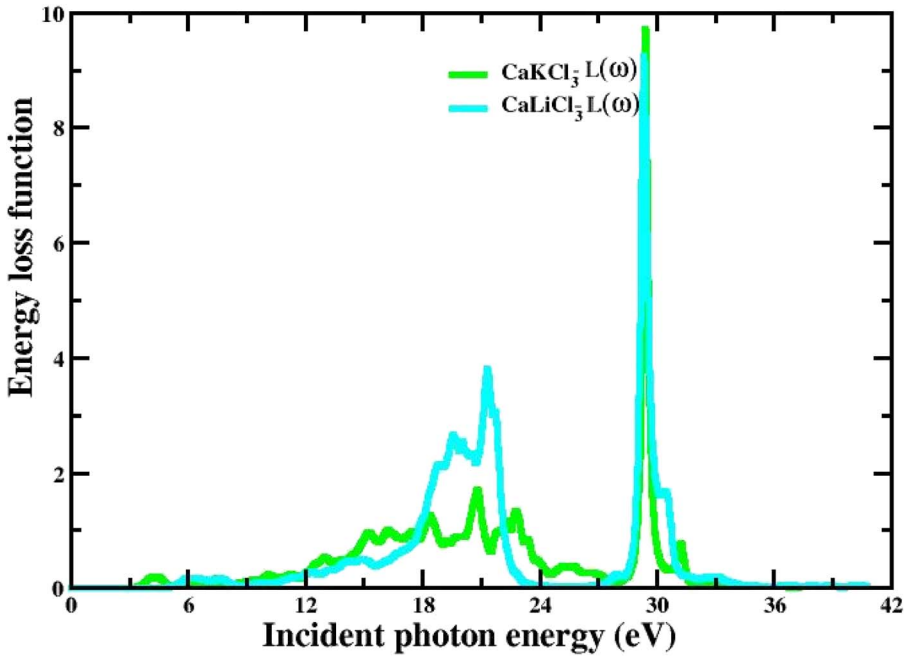

Fig. 11 The computed energy loss function for $CaQCl_3$ (Q = Li and K) chloroperovskites.

modulus Voigt and Reuss approximations, Young's modulus, Passion's ratio, and anisotropy factor:

$$G = \frac{1}{2}(G_V + G_R) \quad (9)$$

$$G_V = \frac{1}{5}(C_{11} - C_{12} + 3C_{44}) \quad (10)$$

$$G_R = \frac{5C_{44}(C_{11} - C_{12})}{4C_{44} + 3(C_{11} - C_{12})} \quad (11)$$

$$E = \frac{9GB}{3B + G} \quad (12)$$

$$\nu = \frac{3B - 2G}{2(3B + G)} \quad (13)$$

$$A = 2C_{44}/(C_{11} - C_{12}) \quad (14)$$

where, G, G_V, G_R, E, ν, and A are the shear modulus, Voigt shear modulus, Reuss shear modulus, Young's modulus, Passion's ratio, and the anisotropy factor respectively.

The rigidity of a material can be determined from the investigated values of "B" (bulk modulus), "G" (shear modulus), and "E" (Young's modulus). The computed values of B, E, and G are tabulated in Table 2 and the values predict that both the ternary chloroperovskites $CaQCl_3$ (Q = Li and K) compounds are rigid and possess hardness to scratch. To evaluate the fragility and ductility of a material, the Passion's ratio"ν", is an important parameter. The values of "ν" investigated for both materials are 1.23 for $CaLiCl_3$ and 1.78 for $CaKCl_3$, which suggests that the selected materials are ductile. Another crucial parameter is the Pugh ratio, which determines the brittle or ductile nature of a material. The threshold value for "B/G" (Pugh ratio) is 1.75.[58] A material will display a brittle nature if the value of the Pugh ratio is less than 1.75, whereas the greater value shows a ductile nature. As in this work, for both materials, the values of "B/G" is 2.84 for $CaLiCl_3$ and 2.52 for $CaKCl_3$. These computed values for selected chloroperovskites predict that the compounds are ductile. The predicted value of anisotropy factor "A" determine whether the material is isotropic or anisotropic, and its critical value is "1" for isotropic whereas a value below or above "1" indicate anisotropy. The values computed for these chloroperovskites are 2.33 for $CaLiCl_3$ and 1.94 for $CaKCl_3$ and show that both compounds are anisotropic. The Cauchy pressure is also another parameter that determines the ductility of a material. The greater positive value of Cauchy pressure indicates ductility.

Table 2 The investigated elastic parameters, including the elastic constant(C_{11}, C_{12}, C_{44} in GPa), the bulk modulus "B", shear modulus "G", Young's modulus "E" and the Cauchy pressure in GPa, the Passion's ratio"ν", the anisotropy factor "A", the Pugh ratio "B/G" for ternary $CaQCl_3$ (Q = Li and K) chloroperovskites compounds

Elastic parameters	$CaLiCl_3$	$CaKCl_3$
C_{11}	64.84	87.74
C_{12}	45.76	56.26
C_{44}	32.56	38.86
B	78.34	81.96
G	27.52	32.45
E	53.33	48.71
ν	1.23	1.78
A	2.33	1.94
Cauchy pressure ($C_{12} - C_{44}$)	13.20	17.40
B/G	2.84	2.52

The computed values of Cauchy pressure are 13.20 GPa for $CaLiCl_3$ and 17.40 GPa for $CaKCl_3$, as can be seen in Table 2.

4. Conclusion

In the current research, the structural, electronic, elastic, and optical properties of ternary chloroperovskites $CaQCl_3$ (Q = Li and K) compounds in the cubic phase are investigated using DFT utilizing the GGA and TB-mBJ approximation within the WIEN2K simulation package. To our best knowledge, there is no available research for these selected perovskites and the key results found through the computational approach are:

• The ternary chloroperovskites $CaQCl_3$ (Q = Li and K) compounds are in the cubic phase and the obtained negative values of formation energy for both compounds indicate that the material is structurally stable and can be experimentally synthesized.

• The analysis of electronic properties (band structure and DOS) shows an indirect nature from "*M–Γ*" with a band gap "E_g" of 4.6 eV for $CaLiCl_3$ and thus acts as an insulator, whereas, the band structure analysis for $CaKCl_3$ depicts a direct nature from "*M–M*" with a band gap "E_g" of 3.3 eV and display the nature of wide band gap semiconductor.

• Elastic properties computed through the IRelast package depict that the compounds of interest are classified as mechanically stable, ductile, anisotropic, and hard to scratch.

• The various parameters in optical properties within incident photon energy range from 0 eV to 42 eV are investigated and the results show that the $CaQCl_3$ (Q = Li and K) compounds are optically active in UV-region and can be a good candidate for scintillating materials.

Based on the very precise investigations for the $CaQCl_3$ (Q = Li and K), it can be deemed that both materials are applicable in much modern electronic equipment, energy storage devices, semiconducting industries, and as a scintillating material.

Conflicts of interest

There are no conflicts to declare.

Acknowledgements

This research was funded by the Princess Nourah bint Abdulrahman University Researchers Supporting Project number (PNURSP2022R29), Princess Nourah bint Abdulrahman University, Riyadh, Saudi Arabia.

References

1 A. Thatribud, Electronic and optical properties of TiO2 by first-principle calculation (DFT-GW and BSE), *Mater. Res. Express*, 2019, **6**(9), 95021.
2 P. Mishra, D. Singh, Y. Sonvane and R. Ahuja, Excitonic effects in the optoelectronic properties of graphene-like BC monolayer, *Opt. Mater.*, 2020, **110**, 110476.
3 E. Oyeniyi, Electronic and optical properties of Mg3XN (X= P, As, Sb, Bi) antiperovskites: The GW/BSE approach, *Solid State Commun.*, 2022, **355**, 114927.
4 L. Zhang, J. Miao, J. Li and Q. Li, Halide perovskite materials for energy storage applications, *Adv. Funct. Mater.*, 2020, **30**(40), 2003653.
5 M. Husain, *et al.*, Structural, electronic, elastic, and magnetic properties of $NaQF_3$ (Q = Ag, Pb, Rh, and Ru) flouroperovskites A first-principle outcomes, *Int. J. Energy Res.*, 2022, **46**(3), 2446–2453.
6 A. Habib, *et al.*, Insight into the Exemplary Physical Properties of Zn-Based Fluoroperovskite Compounds $XZnF_3$ (X = Al, Cs, Ga, In) Employing Accurate GGA Approach: A First-Principles Study, *Materials*, 2022, **15**(7), 2669.
7 M. Arif, *et al.*, Density functional theory based study of the physical properties of cesium based cubic halide perovskites $CsHgX_3$ (X = F and Cl), *Int. J. Energy Res.*, 2022, **46**(3), 2467–2476.
8 J. Saddique, *et al.*, Modeling structural, elastic, electronic and optical properties of ternary cubic barium based fluoroperovskites $MBaF_3$ (M = Ga and In) compounds based on DFT, *Mater. Sci. Semicond. Process.*, 2022, **139**, 106345.
9 S. A. Shah, *et al.*, Insight into the exemplary structural, elastic, electronic and optical nature of $GaBeCl_3$ and $InBeCl_3$: a DFT study, *RSC Adv.*, 2022, **12**(13), 8172–8177.
10 S. Riaz, *et al.*, Physical characteristics of $NaTaO_3$ under pressure for electronic devices, *Mater. Sci. Semicond. Process.*, 2021, **133**, 105976.
11 M. Yaseen, *et al.*, Pressure-induced electronic, optical and thermoelectric properties of cubic $SrZrO_3$: DFT investigation, *Phys. B*, 2021, **612**, 412626.
12 M. Yaseen, *et al.*, Strong electron emission from antiferroelectric PLZT (2/95/5) films, *Appl. Phys. Lett.*, 2014, **104**(22), 222913.
13 D. Li, Z. Ji, C. Luo and H. Wang, Studies of electronic structures and optical properties for cubic $SnZrO_3$ and $SnHfO_3$ under pressure, *Ferroelectrics*, 2021, **585**(1), 230–239.
14 N. Erum and M. A. Iqbal, Physical properties of fluorine-based perovskites for vacuum-ultraviolet-transparent lens materials, *Chin. J. Phys.*, 2017, **55**(3), 893–903.
15 S. R. Kumavat, Y. Sonvane, D. Singh and S. K. Gupta, Two-dimensional $CH_3NH_3PbI_3$ with high efficiency and superior carrier mobility: A theoretical study, *J. Phys. Chem. C*, 2019, **123**(9), 5231–5239.
16 S. Kansara, Y. Sonvane, Pn. Gajjar and S. K. Gupta, 2D BeP_2 monolayer: investigation of electronic and optical properties by driven modulated strain, *RSC Adv.*, 2020, **10**(45), 26804–26812.
17 S. Kansara, D. Singh, S. K. Gupta and Y. Sonvane, Density functional Studies of structural, electronic and vibrational properties of palladium oxide, *Solid State Commun.*, 2016, **245**, 36–41.
18 H. Manaa, Y. Guyot and R. Moncorge, Spectroscopic and tunable laser properties of Co^{2+}-doped single crystals, *Phys. Rev. B: Condens. Matter Mater. Phys.*, 1993, **48**(6), 3633.

19 M. C. M. de Lucas, F. Rodriguez and M. Moreno, Excitation and emission thermal shifts in ABF_3: Mn^{2+} perovskites: coupling with impurity vibrational modes, *J. Phys.: Condens. Matter*, 1995, **7**(38), 7535.

20 C. N. Avram, M. G. Brik, I. Tanaka and N. M. Avram, Electron–phonon interaction in the V^{2+}: $CsCaF_3$ laser crystal: geometry of the $[VF_6]^{4-}$ complex in the $^4T_{2g}$ excited state, *Phys. B*, 2005, **355**(1–4), 164–171.

21 J. M. Garcia-Lastra, J. Y. Buzare, M. T. Barriuso, J. A. Aramburu and M. Moreno, 3 d impurities in normal and inverted perovskites: Differences are not explained by ligand field theory, *Phys. Rev. B: Condens. Matter Mater. Phys.*, 2007, **75**(15), 155101.

22 S. Shahrokhi, *et al.*, Emergence of ferroelectricity in halide perovskites, *Small Methods*, 2020, **4**(8), 2000149.

23 F. Lahoz, B. Villacampa and R. Alcala, The tetragonal to orthorhombic structural phase transition in $RbCaF_3$ single crystals: Influence on the local environment of different nickel probes, *J. Phys. Chem. Solids*, 1997, **58**(6), 881–892.

24 B. Ghebouli, M. A. Ghebouli and M. Fatmi, Structural, elastic, electronic, optical and thermal properties of cubic perovskite $CsCdF_3$ under pressure effect, *Eur. Phys. J.: Appl. Phys.*, 2011, **53**(3), 30101–30108.

25 R. R. Daniels, G. Margaritondo, R. A. Heaton and C. C. Lin, Experimental study of the electronic structure of $KMgF_3$, *Phys. Rev. B: Condens. Matter Mater. Phys.*, 1983, **27**(6), 3878.

26 O. D. I. Moseley, T. A. S. Doherty, R. Parmee, M. Anaya and S. D. Stranks, Halide perovskites scintillators: Unique promise and current limitations, *J. Mater. Chem. C*, 2021, **9**(35), 11588–11604.

27 N. Kawano, *et al.*, Effect of organic moieties on the scintillation properties of organic–inorganic layered perovskite-type compounds, *Jpn. J. Appl. Phys.*, 2016, **55**(11), 110309.

28 S. R. Kumavat, G. Sachdeva, Y. Sonvane and S. K. Gupta, Structural and compositional properties of 2D $CH_3NH_3PbI_3$ hybrid halide perovskite: a DFT study, *RSC Adv.*, 2022, **12**(40), 25924–25931.

29 L. Maduro, S. E. van Heijst and S. Conesa-Boj, First-Principles Calculation of Optoelectronic Properties in 2D Materials: The Polytypic WS_2 Case, *ACS Phys. Chem. Au*, 2022, **2**(3), 191–198.

30 P. Lecoq, Development of new scintillators for medical applications, *Nucl. Instrum. Methods Phys. Res., Sect. A*, 2016, **809**, 130–139.

31 J. Glodo, Y. Wang and R. Shawgo, New developments in scintillators for security applications, *Phys. Procedia*, 2017, **90**, 285–290.

32 S. K. Mathanker, P. R. Weckler and N. Wang, Terahertz (THz) applications in food and agriculture: A review, *Trans. ASABE*, 2013, **56**(3), 1213–1226.

33 M. Güdel and Y. Nazé, X-ray spectroscopy of stars, *Astron. Astrophys. Rev.*, 2009, **17**(3), 309–408.

34 A. C. Ulpe and T. Bredow, GW-BSE Calculations of Electronic Band Gap and Optical Spectrum of $ZnFe_2O_4$: Effect of Cation Distribution and Spin Configuration, *ChemPhysChem*, 2020, **21**(6), 546–551.

35 S. R. Kumavat, Y. Sonvane and S. K. Gupta, Structural, optical, transport, and solar cell properties of 2D halide perovskite $MAZX_3$ (Z = Pb, Sn, and X = Cl, Br, I), *J. Appl. Phys.*, 2020, **128**(11), 114304.

36 M. N. Murshed, M. E. El Sayed, S. Naji and A. Samir, Electronic and optical properties and upper light yield estimation of new scintillating material $TlMgCl_3$: *Ab initio* study, *Results Phys.*, 2021, **29**, 104695.

37 S. Khan, S. U. Zaman, R. Ahmad, N. Mehmood, M. Arif and H. J. Kim, *Ab initio* investigations of structural, elastic, electronic and optical properties of the fluoroperovskite $TlXF_3$ (X = Ca, Cd, Hg, and Mg) compounds, *Mater. Res. Express*, 2020, **6**(12), 125923.

38 Q. V Phan, H. J. Kim, G. Rooh and S. H. Kim, Tl_2ZrCl_6 crystal: Efficient scintillator for X-and γ-ray spectroscopies, *J. Alloys Compd.*, 2018, **766**, 326–330.

39 M. Yaseen, *et al.*, Phase transition and thermoelectric properties of cubic $KNbO_3$ under pressure: DFT approach, *J. Mater. Res. Technol.*, 2021, **11**, 2106–2113.

40 F. Shakoor, *et al.*, Physical characteristics of barium based cubic perovskites, *Chem. Phys. Lett.*, 2021, **779**, 138835.

41 S. Mubashir, *et al.*, Pressure induced electronic, optical and thermoelectric properties of cubic $BaZrO_3$: A first principle calculations, *Optik*, 2021, **239**, 166694.

42 P. Blaha, K. Schwarz, G. K. H. Madsen, D. Kvasnicka, and J. Luitz, *"wien2k," An Augment. Pl. wave+ local orbitals Progr. Calc. Cryst. Prop.*, vol. 60, 2001.

43 L. J. Sham and W. Kohn, One-particle properties of an inhomogeneous interacting electron gas, *Phys. Rev.*, 1966, **145**(2), 561.

44 J. Tao, J. P. Perdew, H. Tang and C. Shahi, Origin of the size-dependence of the equilibrium van der Waals binding between nanostructures, *J. Chem. Phys.*, 2018, **148**(7), 74110.

45 M. Jamal, M. Bilal, I. Ahmad and S. Jalali-Asadabadi, IRelast package, *J. Alloys Compd.*, 2018, **735**, 569–579.

46 D. Koller, F. Tran and P. Blaha, Merits and limits of the modified Becke–Johnson exchange potential, *Phys. Rev. B: Condens. Matter Mater. Phys.*, 2011, **83**(19), 195134.

47 E. Sakalauskas, *et al.*, Dielectric function and optical properties of Al-rich AlInN alloys pseudomorphically grown on GaN, *J. Phys. D: Appl. Phys.*, 2010, **43**(36), 365102.

48 A. Kokalj, XCrySDen—a new program for displaying crystalline structures and electron densities, *J. Mol. Graphics Modell.*, 1999, **17**(3–4), 176–179.

49 A. Vaught, Graphing with Gnuplot and Xmgr: two graphing packages available under linux, *Linux J.*, 1996, **1996**(28es), 7.

50 P. M. Edwards, Origin 7.0: scientific graphing and data analysis software, *J. Chem. Inf. Comput. Sci.*, 2002, **42**(5), 1270–1271.

51 H. Wainer, Visual Revelations: Elegance, Grace, Impact, and Graphical Displays, *Chance*, 1991, **4**(4), 45–47.

52 F. D. Murnaghan, The compressibility of media under extreme pressures, *Proc. Natl. Acad. Sci. U. S. A.*, 1944, **30**(9), 244.

53 S. Bouhmaidi, A. Marjaoui, A. Talbi, M. Zanouni, K. Nouneh and L. Setti, A DFT study of electronic, optical and

thermoelectric properties of Ge-halide perovskites CsGeX3 (X= F, Cl and Br), *Comput. Condens. Matter*, 2022, e00663.

54 Q. Mahmood, *et al.*, Study of new lead-free double perovskites halides Tl_2TiX_6 (X = Cl, Br, I) for solar cells and renewable energy devices, *J. Solid State Chem.*, 2022, **308**, 122887.

55 M. A. Khan, H. A. Alburaih, N. A. Noor and A. Dahshan, Comprehensive investigation of Opto-electronic and transport properties of Cs_2ScAgX_6 (X = Cl, Br, I) for solar cells and thermoelectric applications, *Sol. Energy*, 2021, **225**, 122–128.

56 M. Born, On the stability of crystal lattices. I, *Math. Proc. Cambridge Philos. Soc.*, 1940, **36**(2), 160–172.

57 R. Hill, The elastic behaviour of a crystalline aggregate, *Proc. Phys. Soc., London, Sect. A*, 1952, **65**(5), 349.

58 S. F. Pugh, XCII. Relations between the elastic moduli and the plastic properties of polycrystalline pure metals, *London, Edinburgh Dublin Philos. Mag. J. Sci.*, 1954, **45**(367), 823–843.